.

Supplemental Materials for Curvature-induced motion of a thin Bingham layer in airways bifurcations.

Cyril Karamaoun,[1] Haribalan Kumar,[2] Médéric Argentina,[3] Didier Clamond,[1] and Benjamin Mauroy[4,*]

[1] *Université Côte d'Azur, LJAD, VADER Center, Nice, France*
[2] *Auckland Bioengineering Institute, Auckland, New-Zealand*
[3] *Université Côte d'Azur, Institut de Physique de Nice, VADER Center, Nice, France*
[4] *Université Côte d'Azur, CNRS, LJAD, VADER Center, Nice, France*

(Dated: June 2, 2022)

CONTENTS

* benjamin.mauroy@unice.fr

I. ANALYSIS IN A FRACTAL TREE

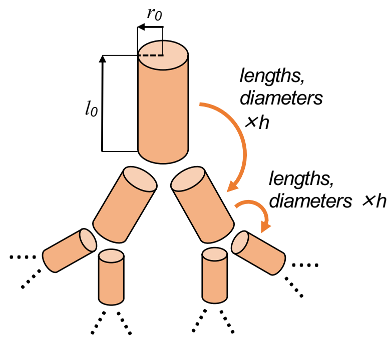

FIG. 1. Fractal model of the bronchial tree used in the qualitative analysis. The size of the branches is decreasing at each bifurcation by a factor $h = (1/2)^{\frac{1}{3}}$. The radius and length of the root of the tree (trachea) are respectively r_0 and l_0.

We search for a qualitative estimation of the pressures induced by the surface tension in the generations of the airway tree. The geometry of the bronchial tree is approximated with a cascade of bifurcating cylindrical airways [8, 9], see Fig. 1. The airways are numbered by using a generation index i that represents the number of bifurcations from the root of the tree, i.e. the trachea, to the considered airway. We assume that the dimensions of the airways between two consecutive generations are related by a homothetic factor h, independent of the generation index. The theoretical value $h = (1/2)^{1/3} \simeq 0.79$ has been found to represent adequately the geometry of the mammal lung [9, 11–15].

We assume that the mucus layer in this geometry has a negligible thickness relatively to the airways radii [5, 14]. Then, the principal curvatures of the air–Bingham fluid interface in the generation i can be assimilated to the cylindrical airway principal curvatures: $1/r_i$ in the radial direction and 0 in the axial direction. These curvatures induce a Laplace pressure drop $p_{L,i}$ between the air and the Bingham fluid:

$$p_{L,i} = -\frac{\gamma}{r_i}$$

Since the airways are considered as perfect cylinders, the radius within a single bronchus does not vary. Thus, there is no gradient of Laplace pressure and the Bingham fluid is motionless. However, the radii vary between the airways, as the distal (deep) bronchi are smaller than the proximal (upper) ones. Because of this change of curvature, the amplitude of the pressure drop increases with the generation index. This implies that a pressure gradient exists between two successive generations, which are connected through bifurcations.

Between two successive generations i and $i+1$, the radii r_i and r_{i+1} relate as $r_{i+1} = h \times r_i$. Assuming that the length of the bifurcation Δx is of the order of magnitude of the airway radius, the curvature radius gradient between two successive generations can be approximated by $\frac{\Delta r_i}{\Delta x} \simeq \frac{h \times r_i - r_i}{r_i} = (h-1) < 0$. Hence, as in [7], the mean shear stress applied to the layer by the pressure drop between two successive generations i and $i+1$ can be qualitatively evaluated to

$$\sigma \simeq \frac{\Delta p_{L,i}}{\Delta x}\frac{\tau}{2} \simeq \gamma \frac{h-1}{r_0^2 h^{2i}}\frac{\tau}{2} < 0$$

If this stresses overcomes the yield stress σ_y, the Bingham fluid flows. Because Σ_{rx} is negative, the Bingham fluid should flow toward the distal regions of the tree, opposite to the direction of the mucociliary clearance.

The previous analysis suggests that the Laplace pressure gradients should be stronger in the distal bifurcations than in the proximal bifurcations. However, a more refined analysis is needed in order to get proper estimations of those gradients and to determine if they can induce shear stresses high enough to overcome the yield stress of the Bingham fluid.

II. LUBRICATION THEORY, BINGHAM CASE

A. Local coordinates system

Coordinates change.
In order to derive the main components of the velocity in the Bingham layer, we will use a lubrication technic based

on the hypothesis that the thickness of the layer τ is far smaller than the characteristic length of the domain [1]. This characteristic length is estimated using the characteristic curvature radius R of the surface on which the layer spreads. Typically, this characteristic curvature radius corresponds to the radius of the airway considered.

The first step is to use a local coordinates system. We will denote (x, y, z) the physical coordinates and (ξ_1, ξ_2, ξ_3) the local coordinates system, as schematized in Fig. 2.

$$(x, y, z) \longrightarrow (\xi_1, \xi_2, \xi_3)$$

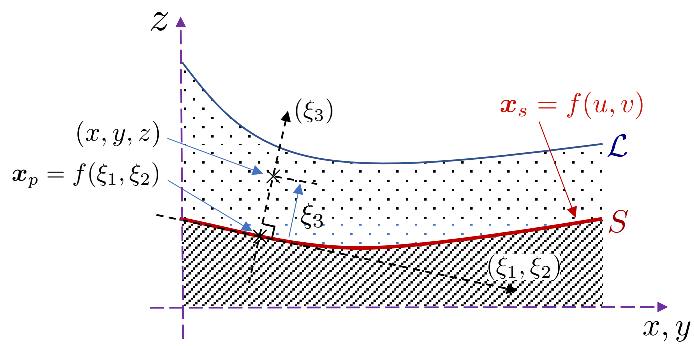

FIG. 2. Transformation from global coordinates $\boldsymbol{x} = (x, y, z)$ to local coordinates $\boldsymbol{\xi} = (\xi_1, \xi_2, \xi_3)$. The plane $(\xi_1\xi_2)$ is tangent to the wall S defined by the surface $\boldsymbol{x}_S = f(u, v)$, where (u, v) is a set of curvilinear coordinates. The direction (ξ_3) is normal to S. The surface $\mathcal{L}$ represents the air–Bingham fluid interface.

We will consider a thin layer that stands on a substrate. The surface S of the substrate is represented locally by a parametric representation $\boldsymbol{x}_S = f(u, v)$, where $(u, v) \in \Omega$ is a curvilinear parameterization of the surface and Ω a subset of $\mathbb{R}^2$. In this case, we can project a point $\boldsymbol{x} = (x, y, z)$ in the layer onto the substrate surface, see Fig. 2. The resulting projection point on the surface is denoted $\boldsymbol{x}_p = f(\xi_1, \xi_2)$. Then,

$$\boldsymbol{x} = f(\xi_1, \xi_2) + \xi_3 \ \boldsymbol{n}_S$$

with

$$\boldsymbol{n}_S = \left(\frac{\partial f}{\partial u} \wedge \frac{\partial f}{\partial v}\right) \Big/ \left|\left|\frac{\partial f}{\partial u} \wedge \frac{\partial f}{\partial v}\right|\right|$$

The new coordinates system is then determined by the triplet $\boldsymbol{\xi} = (\xi_1, \xi_2, \xi_3)$.

We will now use a dimensionless formulation of the equations in order to characterize the dominant velocity of the mucus when $\epsilon = \tau/R$ is small relatively to 1. The ratio ϵ represents the thickness of the mucus layer relatively to the curvature of the airways.

We define dimensionless coordinates associated to the triplet $\boldsymbol{\xi} = (\xi_1, \xi_2, \xi_3)$ using the new triplet $\tilde{\boldsymbol{\xi}} = (\tilde{\xi}_1, \tilde{\xi}_2, \tilde{\xi}_3)$ with $\xi_1 = R\tilde{\xi}_1$, $\xi_2 = R\tilde{\xi}_2$ and $\xi_3 = \tau\tilde{\xi}_3$. In the following, the notation with a tilde over a letter indicates a dimensionless quantity.

- Since f defines the airway wall, we assume that the characteristic size of f is also R and we define $\tilde{f}$ as $f(u, v) = R\tilde{f}(\tilde{u}, \tilde{v})$ with $\tilde{u} = u/R$ and $\tilde{v} = v/R$.

- The Laplace pressure is normalized based on $P = \gamma/R$ and $\tilde{p}_L = p_L/P$. Moreover, for newtonian fluids, the velocity is proportional to $\frac{\gamma}{\mu}\epsilon^2$, hence we choose the scaling $U = \frac{\gamma}{\mu}\epsilon^2$ for the velocity components in ξ_1 and ξ_2 directions. In the ξ_3 direction, the scaling of the velocity is $W = U\tau/R = U\epsilon$.

- Stresses are rescaled with $\sigma^{*3} = \mu\frac{U}{\tau}\tilde{\sigma}^{*3}$ for $* = 1$ or 2, and the other components are rescaled with $\sigma_* = \mu\frac{U}{R}\tilde{\sigma}*$ for $* = 11$, 22, 33 and 12. We denote $\Sigma_{i,j}$ the rescaled value of σ^{ij}.

- Strains are rescaled accordingly, i.e. as σ/μ.

- We assume that all dimensionless variables can decompose into a series relatively to ϵ, i.e. for a variable $*$, its decomposition writes $* = *_0 \ \epsilon^0 + *_1 \ \epsilon + *_2 \ \epsilon^2 + \ldots$.

B. Metric

We define the matrix $C = (c_{i,j})_{i,j} = (\boldsymbol{b}_1, \boldsymbol{b}_2, \boldsymbol{b}_3)$ with

$$\begin{aligned}
\boldsymbol{b}_1 &= \tfrac{\partial \boldsymbol{x}}{\partial \xi_1} = \tfrac{\partial f}{\partial u} + \xi_3 \tfrac{\partial \boldsymbol{n}_S}{\partial u} = \tfrac{\partial \tilde{f}}{\partial \tilde{u}} + \epsilon \tilde{\xi}_3 \tfrac{\partial \boldsymbol{n}_S}{\partial \tilde{u}} \\
\boldsymbol{b}_2 &= \tfrac{\partial \boldsymbol{x}}{\partial \xi_2} = \tfrac{\partial f}{\partial v} + \xi_3 \tfrac{\partial \boldsymbol{n}_S}{\partial v} = \tfrac{\partial \tilde{f}}{\partial \tilde{v}} + \epsilon \tilde{\xi}_3 \tfrac{\partial \boldsymbol{n}_S}{\partial \tilde{v}} \\
\boldsymbol{b}_3 &= \tfrac{\partial \boldsymbol{x}}{\partial \xi_3} = \boldsymbol{n}_S
\end{aligned}$$

and the matrix $\bar{C} = (\bar{c}_{i,j})_{i,j} = C^{-1} = (\boldsymbol{b}^1, \boldsymbol{b}^2, \boldsymbol{b}^3)$. We denote C^0 and $\tilde{C}^0$ the first term of the development of C and $\tilde{C}$ in ϵ.

The associated metric tensor is defined with $g_{(i,j)} = (\boldsymbol{b}_i.\boldsymbol{b}_j)_{i,j}$ and its inverse with $g^{(i,j)} = (\boldsymbol{b}^i.\boldsymbol{b}^j)_{i,j}$. The metric tensors can be rewritten in dimensionless coordinates:

$$g_{(i,j)}(\xi_1, \xi_2, \xi_3) = \tilde{g}_{(i,j)}(\tilde{\xi}_1, \tilde{\xi}_2, \tilde{\xi}_3) = \begin{pmatrix} \left\| \frac{\partial \tilde{f}}{\partial \tilde{u}} \right\|^2 & \frac{\partial \tilde{f}}{\partial \tilde{u}} \cdot \frac{\partial \tilde{f}}{\partial \tilde{v}} & 0 \\ \frac{\partial \tilde{f}}{\partial \tilde{u}} \cdot \frac{\partial \tilde{f}}{\partial \tilde{v}} & \left\| \frac{\partial \tilde{f}}{\partial \tilde{v}} \right\|^2 & 0 \\ 0 & 0 & 1 \end{pmatrix} + O(\epsilon)$$

and

$$g^{(i,j)}(\xi_1, \xi_2, \xi_3) = \tilde{g}^{(i,j)}(\tilde{\xi}_1, \tilde{\xi}_2, \tilde{\xi}_3) = \frac{1}{\tilde{d}(\tilde{u}, \tilde{v})} \begin{pmatrix} \left\| \frac{\partial \tilde{f}}{\partial \tilde{u}} \right\|^2 & -\frac{\partial \tilde{f}}{\partial \tilde{u}} \cdot \frac{\partial \tilde{f}}{\partial \tilde{v}} & 0 \\ -\frac{\partial \tilde{f}}{\partial \tilde{u}} \cdot \frac{\partial \tilde{f}}{\partial \tilde{v}} & \left\| \frac{\partial \tilde{f}}{\partial \tilde{v}} \right\|^2 & 0 \\ 0 & 0 & \tilde{d}(\tilde{u}, \tilde{v}) \end{pmatrix} + O(\epsilon)$$

with $\tilde{d}(\tilde{u}, \tilde{v})$ the determinant of the first term $\tilde{C}^0$ of the development in series of the matrix $\tilde{C}$, $\tilde{d}(\tilde{u}, \tilde{v}) = \left\| \frac{\partial \tilde{f}}{\partial \tilde{u}} \right\|^2 \left\| \frac{\partial \tilde{f}}{\partial \tilde{v}} \right\|^2 - \left(\frac{\partial \tilde{f}}{\partial \tilde{u}} \cdot \frac{\partial \tilde{f}}{\partial \tilde{v}} \right)^2$.

For the sake of notation simplicity, we assume in the following that g^{ij}, g_{ij}, $\tilde{g}^{ij}$ and $\tilde{g}_{ij}$ refer to the coeffcient associated to ϵ^0 in their decomposition in powers of ϵ.

C. Christoffel symbols of the second kind

The Christoffel symbols of the second kind Γ^j_{ik} allow to compute the derivatives in the local coordinates system (ξ_1, ξ_2, ξ_3). The symbols are written, using Einstein notation,

$$\Gamma^k_{ij} = \frac{1}{2} g^{ip} \left(\frac{\partial g_{pj}}{\partial \xi_k} + \frac{\partial g_{pk}}{\partial \xi_j} - \frac{\partial g_{jk}}{\partial \xi_p} \right)$$

We define normalized versions of the Christoffel symbols according to the dimensionless coordinates defined above:

$$\tilde{\Gamma}^k_{i,j} = R\, \Gamma^k_{i,j}$$

The terms in ϵ^0 in the developments in series of the metric tensors $\tilde{g}^{(i,j)}$ and $\tilde{g}_{(i,j)}$ do not depend on $\tilde{\xi}_3$ and have several null terms in their expression Moreover, we have $g_{3,3} = 1$. With these properties, we can get information on the developments in series of the Christoffel symbols relatively to ϵ:

$$\begin{aligned}
\tilde{\Gamma}^k_{i,j} &= O(\epsilon) \;\; \text{if at least one of } i,\ j \text{ or } k \text{ is equal to 3} \\
\tilde{\Gamma}^k_{i,j} &= O(1) \;\; \text{otherwise}
\end{aligned} \tag{1}$$

D. Equations of the mucus dynamics

We assume that the layer stands on the airway wall S. The air–fluid interface is denoted $\mathcal{L}$. The mucus dynamics equations in the coordinates frame (x, y, z) are

$$\begin{cases} \rho\frac{\partial \boldsymbol{u}}{\partial t} - \nabla\cdot\Sigma = \nabla p & \text{in the layer} \\ \nabla\cdot\boldsymbol{u} = 0 & \text{in the layer} \\ \Sigma\cdot\boldsymbol{n} - p\,\boldsymbol{n} = p_L\,\boldsymbol{n} & \text{at the air–fluid interface } \mathcal{L} \\ \boldsymbol{u} = 0 & \text{on the airway wall } S \\ \frac{\partial \boldsymbol{x}}{\partial t} = (\boldsymbol{u}(\boldsymbol{x})\cdot\boldsymbol{n})\,\boldsymbol{n} & \text{at the air–fluid interface } \mathcal{L}\text{, for } \boldsymbol{x}\in\mathcal{L} \\ p_L = -2\gamma\kappa(\boldsymbol{x}, t) & \text{at the air–fluid interface } \mathcal{L} \end{cases} \tag{2}$$

We decompose these equations in the coordinates system $(\boldsymbol{b}_1, \boldsymbol{b}_2, \boldsymbol{b}_3)$. The coordinates of the velocity $\boldsymbol{u}$ in that frame is (u^1, u^2, u^3). The covariant differentiation of a quantity $*$ relatively to the coordinate on the component $\boldsymbol{b}_j$ is denoted $*_{,j}$, and

$$\begin{aligned} &p_{,j} = g^{ji}\frac{\partial p}{\partial \xi_i} \\ &\text{div}_{co}\ \Sigma = \sum_{j=1}^{3}\left(\frac{\partial \sigma^{ij}}{\partial \xi_i} + \Gamma^i_{il}\sigma^{lj} + \Gamma^j_{il}\sigma^{il}\right)\boldsymbol{b}_j \\ &\frac{\partial \boldsymbol{u}}{\partial t} = \sum_{j=1}^{3}\frac{\partial u^j}{\partial t}\boldsymbol{b}_j \end{aligned}$$

For any $j\in\{1, 2, 3\}$, the component of the equation on $\boldsymbol{b}_j$ is

$$\rho\frac{\partial u^j}{\partial t} - \left(\frac{\partial \sigma^{ij}}{\partial \xi_i} + \Gamma^i_{il}\sigma^{lj} + \Gamma^j_{il}\sigma^{il}\right) + g^{ji}\frac{\partial p}{\partial \xi_i} = 0$$

Finally, we can write the stress tensor as

$$\Sigma = \frac{\mu U}{R}\tilde{\Sigma} \ \text{ with } \ \tilde{\Sigma} = \begin{pmatrix} \tilde{\sigma}^{11} & \tilde{\sigma}^{12} & \frac{1}{\epsilon}\tilde{\sigma}^{13} \\ \tilde{\sigma}^{12} & \tilde{\sigma}^{22} & \frac{1}{\epsilon}\tilde{\sigma}^{23} \\ \frac{1}{\epsilon}\tilde{\sigma}^{13} & \frac{1}{\epsilon}\tilde{\sigma}^{23} & \tilde{\sigma}^{33} \end{pmatrix} \tag{3}$$

E. Air–mucus interface $\mathcal{L}$

The air–mucus interface $\mathcal{L}$ is defined in the coordinates system (ξ_1, ξ_2, ξ_3) as

$$\mathcal{L} = \{X_{\mathcal{L}} = g(u, v) = f(u, v) + \tau\,(1 + \eta(u, v, t))\,\boldsymbol{n}_S(u, v)\,|(u, v)\in\Omega\}$$

where η is a function from Ω such that $\eta = o\left(\frac{1}{\epsilon}\right)$, i.e. $\epsilon\times\eta \underset{\epsilon\to 0}{\longrightarrow} 0$. Hence, the order of magnitude of η is at most 1. Moreover, we assume that the layer cannot be of negative thickness and $\eta \geq -1$.

The normal to the air–mucus interface can then be defined as

$$\boldsymbol{n}_{\mathcal{L}} = \left(\frac{\partial g}{\partial u}\wedge\frac{\partial g}{\partial v}\right)\Bigg/\left|\left|\frac{\partial g}{\partial u}\wedge\frac{\partial g}{\partial v}\right|\right|$$

Using the dimensionless system of coordinates, we normalize g with $\tilde{g}(\tilde{\xi}_1, \tilde{\xi}_2, \tilde{\xi}_3) = g(\xi_1, \xi_2, \xi_3)/R$ and we denote $\tilde{\boldsymbol{n}}_*(\tilde{\xi}_1, \tilde{\xi}_2, \tilde{\xi}_3) = \boldsymbol{n}_*(\xi_1, \xi_2, \xi_3)$ with $* = \mathcal{L}$ for the normal to the surface $\mathcal{L}$ or $* = S$ for the normal to the surface S. We can relate the normals to the surfaces S and $\mathcal{L}$ with

$$\tilde{\boldsymbol{n}}_{\mathcal{L}} = \tilde{\boldsymbol{n}}_S + \epsilon\underbrace{(1 + \tilde{\eta})\frac{\frac{\partial \tilde{f}}{\partial \tilde{u}}\wedge\frac{\partial \boldsymbol{n}_S}{\partial \tilde{v}} - \frac{\partial \tilde{f}}{\partial \tilde{v}}\wedge\frac{\partial \boldsymbol{n}_S}{\partial \tilde{u}}}{\left|\left|\frac{\partial f}{\partial u}\wedge\frac{\partial f}{\partial v}\right|\right|}}_{\tilde{\boldsymbol{m}}_{\mathcal{L}}} + O(\epsilon^2) \tag{4}$$

with $\tilde{\eta}(\tilde{\xi}_1, \tilde{\xi}_2, \tilde{t}) = \eta(\xi_1, \xi_2, t)$.

The air–mucus interface is a surface of equation $\xi_3 = \tau(1 + \eta(\xi_1, \xi_2))$ or, in dimensionless coordinates, $\tilde{\xi}_3 = 1 + \tilde{\eta}(\tilde{\xi}_1, \tilde{\xi}_2)$.

F. Boundary conditions at the air–mucus interface $\mathcal{L}$

Based on equation (4), the boundary condition $\Sigma \cdot \boldsymbol{n}_{\mathcal{L}} - p\,\boldsymbol{n}_{\mathcal{L}} = -p_L\,\boldsymbol{n}_{\mathcal{L}}$ at the air–mucus interface becomes in the dimensionless formulation

$$\tilde{\Sigma} \cdot \tilde{\boldsymbol{n}}_{\mathcal{L}} - \frac{1}{\epsilon^2}\tilde{p}\,\tilde{\boldsymbol{n}}_{\mathcal{L}} = -\frac{1}{\epsilon^2}\tilde{p}_L\,\tilde{\boldsymbol{n}}_{\mathcal{L}}$$

Then, based on the expression of $\tilde{\Sigma}$ in equation (3) and of the normal at the air–mucus interface in equation (4), $\tilde{\boldsymbol{n}}_{\mathcal{L}} = \tilde{\boldsymbol{n}}_S + \epsilon\,\tilde{\boldsymbol{m}}_{\mathcal{L}} + O(\epsilon^2)$, we can derive the following relationships,

- At the order $\frac{1}{\epsilon^2}$: $\tilde{p}^0(\xi_1, \xi_2, 1 + \tilde{\eta}(\xi_1, \xi_2, \tilde{t})) = \tilde{p}_L(\xi_1, \xi_2)$.
- At the order $\frac{1}{\epsilon}$: the boundary condition at $\tilde{\xi}_3 = 1 + \eta(\tilde{\xi}_1, \tilde{\xi}_2, \tilde{t})$ is, at the order $1/\epsilon$:

$$\begin{pmatrix} 0 & 0 & \tilde{\sigma}_0^{13} \\ 0 & 0 & \tilde{\sigma}_0^{23} \\ \tilde{\sigma}_0^{13} & \tilde{\sigma}_0^{23} & 0 \end{pmatrix} \cdot \tilde{\boldsymbol{n}}_S - p_1 \tilde{\boldsymbol{n}}_S - p_0\,\tilde{\boldsymbol{m}}_L = p_L\,\tilde{\boldsymbol{m}}_L$$

  Since $p_0 = p_L$ on the boundary and since, in the coordinate system $(\tilde{\xi}_1, \tilde{\xi}_2, \tilde{\xi}_3)$, $\tilde{\boldsymbol{n}}_S = (0, 0, 1)^t$, we can conclude that

$$\begin{aligned} &\tilde{\sigma}_0^{13}\left(\tilde{\xi}_1, \tilde{\xi}_2, 1 + \tilde{\eta}(\tilde{\xi}_1, \tilde{\xi}_2, \tilde{t}), \tilde{t}\right) = \tilde{\sigma}_0^{23}\left(\tilde{\xi}_1, \tilde{\xi}_2, 1 + \tilde{\eta}(\tilde{\xi}_1, \tilde{\xi}_2, \tilde{t}), \tilde{t}\right) = 0 \\ &\tilde{\sigma}_0^{33}\left(\tilde{\xi}_1, \tilde{\xi}_2, 1 + \tilde{\eta}(\tilde{\xi}_1, \tilde{\xi}_2, \tilde{t}), \tilde{t}\right) - \tilde{p}_1 = 0 \end{aligned} \tag{5}$$

G. Component along $\boldsymbol{b}_3$

On the component $\boldsymbol{b}_3$, the equations reduce to

$$\rho\frac{\partial u^3}{\partial t} - \left(\frac{\partial \sigma^{i3}}{\partial \xi_i} + \Gamma^i_{il}\sigma^{l3} + \Gamma^3_{il}\sigma^{il}\right) + g^{3i}\frac{\partial p}{\partial \xi_i} = 0$$

Then, using $g^{31} = g^{32} = 0$ and $g^{33} = 1$ and formulating the equations in a dimensionless form, we have

$$\begin{aligned} \frac{\rho W}{T}\frac{\partial \tilde{u}^3}{\partial \tilde{t}} &- \left(\frac{\Sigma^{13}}{R}\frac{\partial \tilde{\sigma}^{13}}{\partial \tilde{\xi}_1} + \frac{\Sigma^{l3}}{R}\,\tilde{\Gamma}^1_{1l}\tilde{\sigma}^{l3} + \frac{\Sigma^{1l}}{R}\,\tilde{\Gamma}^3_{1l}\tilde{\sigma}^{1l}\right) \\ &- \left(\frac{\Sigma^{23}}{R}\frac{\partial \tilde{\sigma}^{23}}{\partial \tilde{\xi}_2} + \frac{\Sigma^{l3}}{R}\,\tilde{\Gamma}^2_{2l}\tilde{\sigma}^{l3} + \frac{\Sigma^{2l}}{R}\,\tilde{\Gamma}^3_{2l}\tilde{\sigma}^{2l}\right) \\ &- \left(\frac{\Sigma^{33}}{\tau}\frac{\partial \tilde{\sigma}^{33}}{\partial \tilde{\xi}_3} + \frac{\Sigma^{l3}}{R}\,\tilde{\Gamma}^3_{3l}\tilde{\sigma}^{l3} + \frac{\Sigma^{3l}}{R}\,\tilde{\Gamma}^3_{3l}\tilde{\sigma}^{3l}\right) + \frac{P}{\tau}\frac{\partial \tilde{p}}{\partial \tilde{\xi}_3} = 0 \end{aligned} \tag{6}$$

or, once multiplied by $\frac{R^2}{\mu U}$ for getting dimensionless coefficients in front of the derivatives,

$$\begin{aligned} \overbrace{\frac{\rho R^2}{\mu T}}^{\substack{\text{fixed to 1} \\ \text{with } T = \frac{\rho R^2}{\mu}}} \quad \frac{1}{\epsilon}\frac{\partial \tilde{u}^3}{\partial \tilde{t}} &- \left(\frac{1}{\epsilon}\frac{\partial \tilde{\sigma}^{13}}{\partial \tilde{\xi}_1} + \frac{1}{\epsilon}\,\tilde{\Gamma}^1_{11}\tilde{\sigma}^{13} + \tilde{\Gamma}^3_{11}\tilde{\sigma}^{11} + \frac{1}{\epsilon}\,\tilde{\Gamma}^1_{12}\tilde{\sigma}^{23} + \tilde{\Gamma}^3_{12}\tilde{\sigma}^{12} + \tilde{\Gamma}^1_{13}\tilde{\sigma}^{33} + \frac{1}{\epsilon}\,\tilde{\Gamma}^3_{13}\tilde{\sigma}^{13}\right) \\ &- \left(\frac{1}{\epsilon}\frac{\partial \tilde{\sigma}^{23}}{\partial \tilde{\xi}_2} + \frac{1}{\epsilon}\,\tilde{\Gamma}^2_{21}\tilde{\sigma}^{13} + \tilde{\Gamma}^3_{21}\tilde{\sigma}^{21} + \frac{1}{\epsilon}\,\tilde{\Gamma}^2_{22}\tilde{\sigma}^{23} + \tilde{\Gamma}^3_{22}\tilde{\sigma}^{22} + \tilde{\Gamma}^2_{23}\tilde{\sigma}^{33} + \frac{1}{\epsilon}\,\tilde{\Gamma}^3_{23}\tilde{\sigma}^{23}\right) \\ &- \left(\frac{1}{\epsilon}\frac{\partial \tilde{\sigma}^{33}}{\partial \tilde{\xi}_3} + \frac{1}{\epsilon}\,\tilde{\Gamma}^3_{31}\tilde{\sigma}^{13} + \frac{1}{\epsilon}\,\tilde{\Gamma}^3_{31}\tilde{\sigma}^{31} + \frac{1}{\epsilon}\,\tilde{\Gamma}^3_{32}\tilde{\sigma}^{23} + \frac{1}{\epsilon}\,\tilde{\Gamma}^3_{32}\tilde{\sigma}^{32} + 2\tilde{\Gamma}^3_{33}\tilde{\sigma}^{33}\right) + \underbrace{\frac{PR}{\mu U}}_{=1/\epsilon^2}\frac{1}{\epsilon}\frac{\partial \tilde{p}}{\partial \tilde{\xi}_3} = 0 \end{aligned} \tag{7}$$

Since we have shown that all the dimensionless Christoffel symbols are at least $O(1)$ in ϵ, the equations at the order ϵ^{-3} reduce to $\frac{\partial \tilde{p}_0}{\partial \tilde{\xi}_3} = 0$, where $\tilde{p}_0$ is the term in ϵ^0 of the development in series relatively to ϵ of $\tilde{p}$. Then, using the boundary condition on the pressure in equation (2),

$$\tilde{p}_0(\tilde{\xi}_1, \tilde{\xi}_2, \tilde{\xi}_3, \tilde{t}) = \tilde{p}_0(\tilde{\xi}_1, \tilde{\xi}_2, 1 + \tilde{\eta}(\tilde{\xi}_1, \tilde{\xi}_2, \tilde{t}), \tilde{t}) = \tilde{p}_L(\xi_1, \xi_2, \tilde{t})$$

At the first order in ϵ, the pressure does not dependent on ξ_3.

At the order ϵ^{-2}, the equations (7) reduce to $\frac{\partial \tilde{p}_1}{\partial \tilde{\xi}_3} = 0$, where $\tilde{p}_1$ is the term in ϵ^1 of the development in series relatively to ϵ of $\tilde{p}$. And we can conclude that $\tilde{p}_1 = 0$ since $\tilde{p} = p_L$ on the air–mucus interface.

H. Component along $\boldsymbol{b}_1$

As for the component $\boldsymbol{b}_3$, the equations on the component $\boldsymbol{b}_1$ reduce to

$$\rho \frac{\partial u^1}{\partial t} - \left(\frac{\partial \sigma^{i1}}{\partial \xi_i} + \Gamma^i_{il} \sigma^{l1} + \Gamma^1_{il} \sigma^{il} \right) + g^{1i} \frac{\partial p}{\partial \xi_i} = 0$$

Or, in dimensionless coordinates and multiplied by $\frac{R^2}{\mu U}$,

$$\begin{aligned}
&\overbrace{\frac{\rho R^2}{\mu T}}^{=1} \frac{\partial \tilde{u}^1}{\partial \tilde{t}} - \left(\frac{\partial \tilde{\sigma}^{11}}{\partial \tilde{\xi}_1} + \tilde{\Gamma}^1_{11} \tilde{\sigma}^{11} + \tilde{\Gamma}^1_{11} \sigma^{11} + \tilde{\Gamma}^1_{12} \tilde{\sigma}^{21} + \tilde{\Gamma}^1_{12} \sigma^{12} + \frac{1}{\epsilon} \overbrace{\tilde{\Gamma}^1_{13}}^{O(\epsilon)} \tilde{\sigma}^{31} + \frac{1}{\epsilon} \overbrace{\tilde{\Gamma}^1_{13}}^{O(\epsilon)} \sigma^{13} \right) \\
&\quad - \left(\frac{\partial \tilde{\sigma}^{21}}{\partial \tilde{\xi}_2} + \tilde{\Gamma}^2_{21} \tilde{\sigma}^{11} + \tilde{\Gamma}^1_{21} \tilde{\sigma}^{21} + \tilde{\Gamma}^2_{22} \tilde{\sigma}^{21} + \tilde{\Gamma}^1_{22} \tilde{\sigma}^{22} + \frac{1}{\epsilon} \overbrace{\tilde{\Gamma}^2_{23}}^{O(\epsilon)} \tilde{\sigma}^{31} + \frac{1}{\epsilon} \overbrace{\tilde{\Gamma}^1_{23}}^{O(\epsilon)} \tilde{\sigma}^{23} \right) \\
&\quad - \left(\frac{1}{\epsilon^2} \frac{\partial \tilde{\sigma}^{31}}{\partial \tilde{\xi}_3} + \overbrace{\tilde{\Gamma}^3_{31}}^{O(\epsilon)} \tilde{\sigma}^{11} + \frac{1}{\epsilon} \overbrace{\tilde{\Gamma}^1_{31}}^{O(\epsilon)} \sigma^{31} + \overbrace{\tilde{\Gamma}^3_{32}}^{O(\epsilon)} \tilde{\sigma}^{21} + \frac{1}{\epsilon} \overbrace{\tilde{\Gamma}^1_{32}}^{O(\epsilon)} \sigma^{32} + \frac{1}{\epsilon} \overbrace{\tilde{\Gamma}^3_{33}}^{O(\epsilon)} \tilde{\sigma}^{31} + \overbrace{\tilde{\Gamma}^1_{33}}^{O(\epsilon)} \sigma^{33} \right) \\
&\quad + \underbrace{\frac{PR}{\mu U}}_{=1/\epsilon^2} \left(\tilde{g}^{11} \frac{\partial \tilde{p}}{\partial \tilde{\xi}_1} + \tilde{g}^{12} \frac{\partial \tilde{p}}{\partial \tilde{\xi}_2} \right) = 0
\end{aligned} \tag{8}$$

Finally, we can extract the term of the equations at the order ϵ^{-2},

$$\frac{\partial \tilde{\sigma}^{31}_0}{\partial \tilde{\xi}_3} = \tilde{g}^{11} \frac{\partial \tilde{p}_0}{\partial \tilde{\xi}_1} + \tilde{g}^{12} \frac{\partial \tilde{p}_0}{\partial \tilde{\xi}_2}$$

where $\tilde{\sigma}^{31}_0$ is the first term of the development in series of $\tilde{\sigma}^{31}$ relatively to ϵ. Since $\tilde{p}_0 = \tilde{p}_L$ does not depend on $\tilde{\xi}_3$, we can integrate the equation using the stress boundary conditions (equation (5)) at the air–mucus interface, i.e. at $\tilde{\xi}_3 = 1 + \tilde{\eta}(\tilde{\xi}_1, \tilde{\xi}_2)$, and get

$$\tilde{\sigma}^{31}_0(\tilde{\xi}_1, \tilde{\xi}_2, \tilde{\xi}_3, \tilde{t}) = - \overbrace{\left(\tilde{g}^{11} \frac{\partial \tilde{p}_L}{\partial \tilde{\xi}_1} + \tilde{g}^{12} \frac{\partial \tilde{p}_L}{\partial \tilde{\xi}_2} \right)}^{\tilde{\partial} \tilde{p}_{L1}} \left(1 + \tilde{\eta}(\tilde{\xi}_1, \tilde{\xi}_2, \tilde{t}) - \tilde{\xi}_3 \right) \tag{9}$$

Doing a similar analysis on the component $\boldsymbol{b}_2$ leads to

$$\tilde{\sigma}^{32}_0(\tilde{\xi}_1, \tilde{\xi}_2, \tilde{\xi}_3, \tilde{t}) = - \underbrace{\left(\tilde{g}^{21} \frac{\partial \tilde{p}_L}{\partial \tilde{\xi}_1} + \tilde{g}^{22} \frac{\partial \tilde{p}_L}{\partial \tilde{\xi}_2} \right)}_{\tilde{\partial} \tilde{p}_{L2}} \left(1 + \tilde{\eta}(\tilde{\xi}_1, \tilde{\xi}_2, \tilde{t}) - \tilde{\xi}_3 \right) \tag{10}$$

For $i = 1, 2$, we define the operator $\tilde{\partial}\tilde{q}_i$ of a quantity $\tilde{q}$ as

$$\tilde{\partial}\tilde{q}_i = \tilde{g}^{i1}\frac{\partial \tilde{q}}{\partial \tilde{\xi}_1} + \tilde{g}^{i2}\frac{\partial \tilde{q}}{\partial \tilde{\xi}_2}$$

Then, we define the operator $\nabla_{\tilde{\xi}}\,\tilde{q}$ of a quantity $\tilde{q}$ as

$$\nabla_{\tilde{\xi}}\,\tilde{q} = \tilde{\partial}\tilde{q}_1\tilde{\boldsymbol{b}}_1 + \tilde{\partial}\tilde{q}_2\tilde{\boldsymbol{b}}_2$$

and $\|\nabla_{\tilde{\xi}}\,\tilde{q}\| = \sqrt{\tilde{g}_{11}(\tilde{\partial}\tilde{q}_1)^2 + \tilde{g}_{22}(\tilde{\partial}\tilde{q}_2)^2 + 2\tilde{g}_{12}\tilde{\partial}\tilde{q}_1\tilde{\partial}\tilde{q}_2}$. Using these notations, we have

$$\begin{aligned}
\tilde{\sigma}_0^{31}(\tilde{\xi}_1, \tilde{\xi}_2, \tilde{\xi}_3, \tilde{t}) &= -\tilde{\partial}\tilde{p}_{L1}\left(1 + \tilde{\eta}(\tilde{\xi}_1, \tilde{\xi}_2, \tilde{t}) - \tilde{\xi}_3\right) \\
\tilde{\sigma}_0^{32}(\tilde{\xi}_1, \tilde{\xi}_2, \tilde{\xi}_3, \tilde{t}) &= -\tilde{\partial}\tilde{p}_{L2}\left(1 + \tilde{\eta}(\tilde{\xi}_1, \tilde{\xi}_2, \tilde{t}) - \tilde{\xi}_3\right)
\end{aligned}$$

Moreover, knowing that $\tilde{p}_1 = 0$, the terms in ϵ^{-1} in the equations (8) and in their equivalent on the component $\boldsymbol{b}_2$ lead to

$$\begin{aligned}
\frac{\partial \tilde{\sigma}_1^{31}}{\partial \tilde{\xi}_3} &= \tilde{g}^{11}\frac{\partial \tilde{p}_1}{\partial \tilde{\xi}_1} + \tilde{g}^{12}\frac{\partial \tilde{p}_1}{\partial \tilde{\xi}_2} = 0 \\
\frac{\partial \tilde{\sigma}_1^{32}}{\partial \tilde{\xi}_3} &= \tilde{g}^{21}\frac{\partial \tilde{p}_1}{\partial \tilde{\xi}_1} + \tilde{g}^{22}\frac{\partial \tilde{p}_1}{\partial \tilde{\xi}_2} = 0
\end{aligned}$$

Consequently, both $\tilde{\sigma}_1^{31}$ and $\tilde{\sigma}_1^{32}$ are independent on $\tilde{\xi}_3$.

I. Curvature

The local curvature of the air–Bingham interface $\mathcal{L}$ parameterized as $\boldsymbol{x} = g(u, v, t) = f(u, v) + \tau(1 + \eta(u, v, t))\,\boldsymbol{n}_S(u, v)$ is

$$\kappa(u, v) = \frac{(1 + \frac{\partial g}{\partial u}^2)\frac{\partial^2 g}{\partial v^2} - 2\frac{\partial g}{\partial u}\frac{\partial g}{\partial v}\frac{\partial^2 g}{\partial u \partial v} + (1 + \frac{\partial g}{\partial v}^2)\frac{\partial^2 g}{\partial u^2}}{(1 + \frac{\partial g}{\partial u}^2 + \frac{\partial g}{\partial v}^2)^{\frac{3}{2}}}$$

Then, if we denote $\tilde{\kappa}(\tilde{u}, \tilde{v}) = R\;\kappa(u, v)$ and use the previously defined dimensionless variables, then

$$\tilde{\kappa}(\tilde{u}, \tilde{v}) = \frac{(1 + \frac{\partial \tilde{f}}{\partial \tilde{u}}^2)\frac{\partial^2 \tilde{f}}{\partial \tilde{v}^2} - 2\frac{\partial \tilde{f}}{\partial \tilde{u}}\frac{\partial \tilde{f}}{\partial \tilde{v}}\frac{\partial^2 \tilde{f}}{\partial \tilde{u}\partial \tilde{v}} + (1 + \frac{\partial \tilde{f}}{\partial \tilde{v}}^2)\frac{\partial^2 \tilde{f}}{\partial \tilde{u}^2}}{(1 + \frac{\partial \tilde{f}}{\partial \tilde{u}}^2 + \frac{\partial \tilde{f}}{\partial \tilde{v}}^2)^{\frac{3}{2}}} + O(\epsilon)$$

with $f(u, v) = R\tilde{f}(\tilde{u}, \tilde{v})$, $\tilde{u} = u/R$, $\tilde{v} = v/R$ and $\epsilon = \tau/R$.

J. Model for mucus rheology

We assume a quasi-static response of the surface tension to curvature changes and assume that the mucus behaves as a Bingham fluid as in [7, 10]. The Bingham viscoplastic constitutive model is

$$\begin{cases} \Sigma = \left(\mu + \frac{\sigma_y}{\dot{\gamma}}\right)\dot{\Gamma} & \text{for } \sigma > \sigma_y \\ \dot{\Gamma} = 0 & \text{for } \sigma \leq \sigma_y \end{cases} \tag{11}$$

with $\dot{\Gamma} = (\dot{\gamma}_{i,j})_{i,j=1\ldots3} = \frac{1}{2}\left(\nabla u + (\nabla u)^t\right)$. The quantities σ and $\dot{\gamma}$ are defined as $\sigma = \sqrt{\frac{1}{2}\Sigma{:}\Sigma}$ and $\dot{\gamma} = \sqrt{\frac{1}{2}\dot{\Gamma}{:}\dot{\Gamma}}$.

These quantities are defined in the coordinate system (x, y, z). Their expression in the coordinate system (ξ_1, ξ_2, ξ_3) are obtained by using the covariant differentiation. Thus, in the coordinates (ξ_1, ξ_2, ξ_3), the derivative relatively to ξ_j of the $\boldsymbol{b}_i$ component u^i of the velocity is

$$u^i_{,j} = \frac{\partial u_i}{\partial \xi_j} + \sum_{k=1}^{3}\Gamma^i_{jk}u^k \tag{12}$$

The dimensionless formulation of this derivative is given by the dimensionless velocities $u_i = U\tilde{u}_i$ for $i = 1, 2$ and $u_3 = U\epsilon\tilde{u}_3$. Then the dimensionless formulation of the covariant derivatives are

$$u^i_{,j} = \tfrac{U}{R}\tilde{u}^i_{,j} \qquad \text{for } i = 1,2 \text{ and } j = 1,2$$

$$u^3_{,j} = \tfrac{U\epsilon}{R}\tilde{u}^3_{,j} \qquad \text{for } j = 1,2$$

$$u^i_{,3} = \tfrac{U}{\tau}\tilde{u}^i_{,3} \qquad \text{for } i = 1,2$$

$$u^3_{,3} = \tfrac{U\epsilon}{\tau}\tilde{u}^3_{,3} = \tfrac{U}{R}\tilde{u}^3_{,3}$$

And,

$$\begin{aligned}
\tilde{u}^i_{,j} &= \tfrac{\partial \tilde{u}^i}{\partial \tilde{\xi}_j} + \underbrace{\tilde{\Gamma}^i_{j1}}_{O(1)}\tilde{u}^1 + \underbrace{\tilde{\Gamma}^i_{j2}}_{O(1)}\tilde{u}^2 + \underbrace{\tilde{\Gamma}^i_{j3}}_{O(\epsilon)}\epsilon\,\tilde{u}^3 = O(1) && \text{for } i = 1,2 \text{ and } j = 1,2\\
\tilde{u}^3_{,j} &= \tfrac{\partial \tilde{u}^3}{\partial \tilde{\xi}_j} + \underbrace{\tilde{\Gamma}^3_{j1}}_{O(\epsilon)}\tilde{u}^1 + \underbrace{\tilde{\Gamma}^3_{j2}}_{O(\epsilon)}\tilde{u}^2 + \underbrace{\tilde{\Gamma}^3_{j3}}_{O(\epsilon)}\epsilon\,\tilde{u}^3 = O(1) && \text{for } j = 1,2\\
\tilde{u}^i_{,3} &= \tfrac{1}{\epsilon}\tfrac{\partial \tilde{u}^i}{\partial \tilde{\xi}_3} + \underbrace{\tilde{\Gamma}^i_{31}}_{O(\epsilon)}\tilde{u}^1 + \underbrace{\tilde{\Gamma}^i_{32}}_{O(\epsilon)}\tilde{u}^2 + \underbrace{\tilde{\Gamma}^i_{33}}_{O(\epsilon)}\epsilon\,\tilde{u}^3 = \tfrac{1}{\epsilon}\tfrac{\partial u^i}{\partial \tilde{\xi}_3} + O(\epsilon) && \text{for } i = 1,2\\
\tilde{u}^3_{,3} &= \tfrac{\partial \tilde{u}^3}{\partial \tilde{\xi}_3} + \underbrace{\tilde{\Gamma}^3_{31}}_{O(\epsilon)}\tilde{u}^1 + \underbrace{\tilde{\Gamma}^3_{32}}_{O(\epsilon)}\tilde{u}^2 + \underbrace{\tilde{\Gamma}^3_{33}}_{O(\epsilon)}\epsilon\,\tilde{u}^3 = O(1)
\end{aligned} \tag{13}$$

We denote now $\dot{\gamma} = \frac{U}{R}\tilde{\dot{\gamma}}$. Then, using the dimensionless Christoffel symbols from equation (1) and rewriting the covariant derivatives from equation (12) in a dimensionless form, we can compute the dominant term in ϵ of the dimensionless shear rate:

$$\tilde{\dot{\gamma}} = \frac{1}{2\epsilon}\overbrace{\tilde{g}_{33}}^{=1}\sqrt{\tilde{g}_{11}\left(\frac{\partial \tilde{u}^1}{\partial \tilde{\xi}_3}\right)^2 + \tilde{g}_{22}\left(\frac{\partial \tilde{u}^2}{\partial \tilde{\xi}_3}\right)^2 + 2\tilde{g}_{12}\frac{\partial \tilde{u}^1}{\partial \tilde{\xi}_3}\frac{\partial \tilde{u}^2}{\partial \tilde{\xi}_3}} + O(1) = \frac{1}{\epsilon}E$$

Similary, for the stress σ with $\sigma = \frac{\mu U}{R}\tilde{\sigma}$,

$$\tilde{\sigma} = \frac{1}{2\epsilon}\overbrace{\tilde{g}_{33}}^{=1}\sqrt{\tilde{g}_{11}\left(\tilde{\sigma}^{13}\right)^2 + \tilde{g}_{22}\left(\tilde{\sigma}^{23}\right)^2 + 2\tilde{g}_{12}\tilde{\sigma}^{13}\tilde{\sigma}^{23}} + O(1) = \frac{1}{\epsilon}T$$

The yield condition $\sigma \geq \sigma_y$ rewrites

$$\tilde{\sigma} \geq \frac{\sigma_y R}{\mu U} = \frac{1}{\epsilon}\frac{\sigma_y \tau}{\mu U} = \frac{1}{\epsilon}\frac{\sigma_y R^2}{\gamma\tau} = \frac{1}{\epsilon}B$$

where $B = \frac{\sigma_y R^2}{\gamma\tau}$ is the Bingham number, that compares the yield stress to the surface tension stress.

Under plastic conditions, i.e. $\epsilon\tilde{\sigma} < B$, we have $\tilde{\dot{\gamma}} = 0$. Under flow conditions, i.e. when $\tilde{\sigma} \geq B/\epsilon$, stress-strain relationships at the order $1/\epsilon$ are

$$\begin{cases}
\tilde{\sigma}^{13}_0 = \dfrac{\partial \tilde{u}^1_0}{\partial \tilde{\xi}_3}\left(1 + \dfrac{B}{E^0}\right) = -\tilde{\partial}\tilde{p}_{L1}(1 + \tilde{\eta} - \tilde{\xi}_3)\\
\tilde{\sigma}^{23}_0 = \dfrac{\partial \tilde{u}^2_0}{\partial \tilde{\xi}_3}\left(1 + \dfrac{B}{E^0}\right) = -\tilde{\partial}\tilde{p}_{L2}(1 + \tilde{\eta} - \tilde{\xi}_3)\\
E^0 = \sqrt{\tilde{g}_{11}\left(\dfrac{\partial \tilde{u}^1_0}{\partial \tilde{\xi}_3}\right)^2 + \tilde{g}_{22}\left(\dfrac{\partial \tilde{u}^2_0}{\partial \tilde{\xi}_3}\right)^2 + 2\tilde{g}_{12}\dfrac{\partial \tilde{u}^1_0}{\partial \tilde{\xi}_3}\dfrac{\partial \tilde{u}^2_0}{\partial \tilde{\xi}_3}}
\end{cases} \tag{14}$$

The first two equations show that u^1_0 and u^2_0 are increasing in amplitude with $\tilde{\xi}_3$ since their $\tilde{\xi}_3$ derivative is positive. We also have $\frac{\partial \tilde{u}^2_0}{\partial \tilde{\xi}_3}\ \tilde{\partial}\tilde{p}_{L1} = \frac{\partial \tilde{u}^1_0}{\partial \tilde{\xi}_3}\ \tilde{\partial}\tilde{p}_{L2}$ and $E^0 = |\frac{\partial \tilde{u}^1_0}{\partial \tilde{\xi}_3}|\ ||\nabla_{\tilde{\xi}}\,\tilde{p}_L||/|\tilde{\partial}\tilde{p}_{L1}| = |\frac{\partial \tilde{u}^2_0}{\partial \tilde{\xi}_3}|\ ||\nabla_{\tilde{\xi}}\,\tilde{p}_L||/|\tilde{\partial}\tilde{p}_{L2}|$, with $||\nabla_{\tilde{\xi}}\,\tilde{p}_L||^2 = \tilde{g}_{11}\tilde{\partial}\tilde{p}^2_{L1} + \tilde{g}_{22}\tilde{\partial}\tilde{p}^2_{L2} + 2\tilde{g}_{12}\tilde{\partial}\tilde{p}_{L1}\tilde{\partial}\tilde{p}_{L2}$.

As the stress is decreasing with ξ_3, if the fluid is liquid at the height $\tilde{\xi}_3$, then it is liquid at the height 0. Hence, integrating equations (14) from 0 to $\tilde{\xi}_3$ and adding the boundary conditions (5) lead to

$$\begin{aligned}\tilde{u}_0^1 &= \frac{1}{2}\tilde{\partial}\tilde{p}_{L1}\;\tilde{\xi}_3\left(\tilde{\xi}_3 - 2\left(1+\tilde{\eta} - \frac{B}{\|\nabla_{\tilde{\xi}}\,\tilde{p}_L\|}\right)\right)\\ \tilde{u}_0^2 &= \frac{1}{2}\tilde{\partial}\tilde{p}_{L2}\;\tilde{\xi}_3\left(\tilde{\xi}_3 - 2\left(1+\tilde{\eta} - \frac{B}{\|\nabla_{\tilde{\xi}}\,\tilde{p}_L\|}\right)\right)\end{aligned} \tag{15}$$

The stress is then

$$\tilde{\sigma}_0 = \frac{1}{\epsilon}\sqrt{\tilde{g}_{11}(\tilde{\sigma}_0^{13})^2 + \tilde{g}_{22}(\tilde{\sigma}_0^{23})^2 + 2\tilde{g}_{12}\tilde{\sigma}_0^{13}\tilde{\sigma}_0^{23}} = \frac{|1+\tilde{\eta}-\tilde{\xi}_3|}{\epsilon} \times \|\nabla_{\tilde{\xi}}\,\tilde{p}_L\|$$

The fluid is flowing when $\tilde{\sigma}_0 \geq \frac{1}{\epsilon}B$ or, similarly, since $\tilde{\xi}_3 \leq 1+\tilde{\eta}$, when

$$\tilde{\xi}_3 \leq \tilde{Z}(\tilde{\xi}_1,\tilde{\xi}_2) = 1 + \tilde{\eta}(\tilde{\xi}_1,\tilde{\xi}_2) - \frac{B}{\|\nabla_{\tilde{\xi}}\,\tilde{p}_L(\tilde{\xi}_1,\tilde{\xi}_2)\|}$$

$\tilde{Z}(\tilde{\xi}_1,\tilde{\xi}_2)$ is the first order yield surface.

Finally, the terms in ϵ^0 of the velocity when $\tilde{\xi}_3 \leq \tilde{Z}(\tilde{\xi}_1,\tilde{\xi}_2) = 1+\tilde{\eta} - \frac{B}{\|\nabla_{\tilde{\xi}}\,\tilde{p}_L\|}$ are

$$\begin{aligned}\tilde{u}_0^1 &= \frac{1}{2}\tilde{\partial}\tilde{p}_{L1}\;\tilde{\xi}_3\left(\tilde{\xi}_3 - 2\left(1+\tilde{\eta} - \frac{B}{\|\nabla_{\tilde{\xi}}\,\tilde{p}_L\|}\right)\right)\\ \tilde{u}_0^2 &= \frac{1}{2}\tilde{\partial}\tilde{p}_{L2}\;\tilde{\xi}_3\left(\tilde{\xi}_3 - 2\left(1+\tilde{\eta} - \frac{B}{\|\nabla_{\tilde{\xi}}\,\tilde{p}_L\|}\right)\right)\end{aligned} \tag{16}$$

K. Dimensional fluid dynamics of the Bingham layer

We recall that the local coordinate system is $(\boldsymbol{b}_1, \boldsymbol{b}_2, \boldsymbol{b}_3)$ and that the metric tensor is $C = (\boldsymbol{b}_i.\boldsymbol{b}_j)_{ij} = (g_{ij})_{ij}$ with its inverse being $C^{-1} = (g^{ij})_{ij}$.

As for the dimensionless case, we define for $i = 1,2$ the operator ∂q_i of a quantity q as

$$\partial q_i = g^{i1}\frac{\partial q}{\partial \xi_1} + g^{i2}\frac{\partial q}{\partial \xi_2} \tag{17}$$

Then, we define the operator $\nabla_\xi\, q$ of a quantity q as

$$\nabla_\xi\, q = \partial q_1 \boldsymbol{b}_1 + \partial q_2 \boldsymbol{b}_2 \tag{18}$$

and

$$\|\nabla_\xi\, q\| = \sqrt{\nabla_\xi\, q \,.\, \nabla_\xi\, q} = \sqrt{g_{11}(\partial q_1)^2 + g_{11}(\partial q_2)^2 + 2g_{12}\partial q_1 \partial q_2} \tag{19}$$

Using these definitions, the dimensional stress is

$$\sigma(\xi_1,\xi_2,\xi_3) = (\tau + \eta - \xi_3)\;\|\nabla_\xi\, p_L\| + O(\epsilon)$$

The yield surface is located at

$$Z(\xi_1,\xi_2) = \tau + \eta - \frac{\sigma_y}{\|\nabla_\xi\, p_L\|} \tag{20}$$

In the yielded region, i.e. where $\xi_3 \leq Z(\xi_1,\xi_2)$, the velocity at height ξ_3 is given by

$$\begin{cases} u^1(\xi_1,\xi_2,\xi_3,t) = -\dfrac{1}{2\mu}\partial p_{L1}\;\xi_3\,(2Z(\xi_1,\xi_2) - \xi_3) + O\,(U\epsilon)\\ u^2(\xi_1,\xi_2,\xi_3,t) = -\dfrac{1}{2\mu}\partial p_{L2}\;\xi_3\,(2Z(\xi_1,\xi_2) - \xi_3) + O\,(U\epsilon)\\ u^3(\xi_1,\xi_2,\xi_3,t) = O(U\epsilon)\end{cases} \tag{21}$$

These results indicate that the normal velocity of the Bingham fluid layer, represented by $\frac{d\boldsymbol{x}}{dt} = u^3(\xi_1, \xi_2, \xi_3, t)\boldsymbol{b}_3$ (equation (2)), is small relatively to the transversal velocities.

Moreover, we can exhibit a criterion on the curvature of the air–fluid interface indicating if the fluid is able to flow or not. This condition corresponds to $Z(\xi_1, \xi_2) > 0$, or, knowing that $p_L(\xi_1, \xi_2) = -2\gamma\kappa(\xi_1, \xi_2)$, to

$$\|\nabla_\xi \kappa(\xi_1, \xi_2)\| < \frac{\sigma_y}{2\gamma(\tau + \eta(\xi_1, \xi_2))} \tag{22}$$

Finally, we denote $\boldsymbol{u}_m = (u_m^1, u_m^2, u_m^3)$ the dominant velocity averaged over the thickness of the layer written in the frame (ξ_1, ξ_2, ξ_3) and:

$$\begin{cases} u_m^1(\xi_1, \xi_2, t) = -\frac{1}{2\mu}\partial p_{L1} \hat{Z}^2(\xi_1, \xi_2)\left(1 - \frac{\hat{Z}(\xi_1, \xi_2)}{3(\tau+\eta)}\right) + O(U\epsilon) \\ u_m^2(\xi_1, \xi_2, t) = -\frac{1}{2\mu}\partial p_{L2} \hat{Z}^2(\xi_1, \xi_2)\left(1 - \frac{\hat{Z}(\xi_1, \xi_2)}{3(\tau+\eta)}\right) + O(U\epsilon) \\ u_m^3(\xi_1, \xi_2, t) = O(U\epsilon) \\ \hat{Z}(\xi_1, \xi_2, t) = \max\left(0, \tau + \eta(\xi_1, \xi_2) - \frac{\sigma_y}{||\nabla_\xi p_L(\xi_1, \xi_2)||}\right) \end{cases}$$

or

$$\boldsymbol{u}_m(\xi_1, \xi_2, t) = -\frac{1}{2\mu}\hat{Z}^2(\xi_1, \xi_2)\left(1 - \frac{\hat{Z}(\xi_1, \xi_2)}{3(\tau + \eta)}\right)\nabla_\xi p_L + O(U\epsilon) \tag{23}$$

In order to compute the integrals on the ξ_3 direction, we used the property that if the fluid is yielded at the height ξ_3, it is yielded at all the heights smaller than ξ_3 since the stress is decreasing with ξ_3. For ξ_3 larger than $Z(\xi_1, \xi_2)$, the layer is solid and its velocity is the same as the velocity at the point $(\xi_1, \xi_2, \hat{Z}(\xi_1, \xi_2))$.

In the main text, we use the quantity $\theta(\xi_1, \xi_2) = \tau + \eta - \hat{Z}(\xi_1, \xi_2)$.

III. VELOCITY OF THE BINGHAM FLUID LAYER AVERAGED OVER A BIFURCATION IN GENERATION i

We assume now that the thickness of the Bingham fluid layer is constant, i.e. $\eta = 0$ in the equations of the previous section. We consider the wall of a bifurcation B_i in the generation i, parameterized by $\boldsymbol{x} = f^i(u, v)$ with $(u, v) \in \Omega_i$. We denote $(\xi_1^i, \xi_2^i, \xi_3^i)$ the local coordinates system in B_i as defined in the Appendix II A. Due to the structure of our model, we know that $(\xi_1^i, \xi_2^i, \xi_3^i) = h^i \times (\xi_1^0, \xi_2^0, \xi_3^0)$. The direction of the mucocilliary clearance is represented by the unit vector $\boldsymbol{t_m}(\xi_1^i, \xi_2^i)$, see the section V of this document. By definition, the component of $\boldsymbol{t_m}$ along ξ_3 is 0. We define the variation of a quantity q in the direction of the mucocilliary clearance with

$$\frac{\partial_\xi q}{\partial m} = \nabla_\xi q(\xi_1^i, \xi_2^i) \cdot \boldsymbol{t_m}(\xi_1^i, \xi_2^i)$$

The Bingham layer velocity in the direction of the mucociliary clearance averaged on the whole bifurcation B_i is

$$V_{m,i} \;= v_{\text{cilia}} - \frac{1}{|B_i|}\frac{1}{2\mu}\int_{B_i \cap \{(\xi_1^i, \xi_2^i) | Z_i(\xi_1^i, \xi_2^i) > 0\}} \frac{\partial_\xi p_L}{\partial m}(\xi_1^i, \xi_2^i)\; Z_i^2(\xi_1^i, \xi_2^i)\left(1 - \frac{Z_i(\xi_1^i, \xi_2^i)}{3\tau}\right) \|\frac{\partial f^i}{\partial u} \wedge \frac{\partial f^i}{\partial v}\| d\xi_1^i d\xi_2^i$$

The condition $Z_i(\xi_1^i, \xi_2^i) > 0$ can be reformulated in $(\xi_1^0, \xi_2^0, \xi_3^0)$ using $Z_0(\xi_1^0, \xi_2^0)$ and i. It becomes $Z_0(\xi_1^0, \xi_2^0) > \tau\left(1 - \frac{1}{h^{2i}}\right)$. Moreover $Z_i(\xi_1^i, \xi_2^i) = \tau - h^{2i}(\tau - Z_0(\xi_1^0, \xi_2^0))$.

Now, we recall that $\nabla_\xi p_{L,i}(\xi_1^i, \xi_2^i) = -2\gamma\nabla_\xi \kappa_i(\xi_1^i, \xi_2^i) = -\frac{2\gamma}{h^{2i}}\nabla_\xi \kappa_0(\xi_1^0, \xi_2^0)$ and we denote

$$D_i = B_0 \cap \left\{(\xi_1^0, \xi_2^0) \mid ||\nabla_\xi \kappa_0(\xi_1^0, \xi_2^0)|| > \frac{\sigma_y}{2\tau\gamma}h^{2i}\right\}$$

Then, we can write the previous equation on $V_{m,i}$ using powers of $\left(\frac{\sigma_y h^{2i}}{2\tau\gamma}\frac{1}{||\nabla_\xi\,\kappa_0(\xi_1^0,\xi_2^0)||}\right)$,

$$\begin{aligned} V_{m,i} = \; & v_{\text{cilia}} \\ & + \frac{1}{h^{2i}}\frac{2\gamma\tau^2}{3\mu|B_0|}\int_{D_i}\frac{\partial_\xi\kappa_0}{\partial m}(\xi_1^0,\xi_2^0)\left(\frac{\sigma_y h^{2i}}{2\tau\gamma}\frac{1}{||\nabla_\xi\,\kappa_0(\xi_1^0,\xi_2^0)||}\right)^0 \left\|\frac{\partial f^0}{\partial u}\wedge\frac{\partial f^0}{\partial v}\right\| d\xi_1^0 d\xi_2^0 \\ & - \frac{1}{h^{2i}}\frac{\gamma\tau^2}{\mu|B_0|}\int_{D_i}\frac{\partial_\xi\kappa_0}{\partial m}(\xi_1^0,\xi_2^0)\left(\frac{\sigma_y h^{2i}}{2\tau\gamma}\frac{1}{||\nabla_\xi\,\kappa_0(\xi_1^0,\xi_2^0)||}\right)^1 \left\|\frac{\partial f^0}{\partial u}\wedge\frac{\partial f^0}{\partial v}\right\| d\xi_1^0 d\xi_2^0 \\ & + \frac{1}{h^{2i}}\frac{\gamma\tau^2}{3\mu|B_0|}\int_{D_i}\frac{\partial_\xi\kappa_0}{\partial m}(\xi_1^0,\xi_2^0)\left(\frac{\sigma_y h^{2i}}{2\tau\gamma}\frac{1}{||\nabla_\xi\,\kappa_0(\xi_1^0,\xi_2^0)||}\right)^3 \left\|\frac{\partial f^0}{\partial u}\wedge\frac{\partial f^0}{\partial v}\right\| d\xi_1^0 d\xi_2^0 \end{aligned} \tag{24}$$

$$\begin{aligned} V_{m,i} = \; & v_{\text{cilia}} + \frac{1}{h^{2i}}\frac{2\gamma\tau^2}{3\mu|B_0|}\int_{B_0\cap\{(\xi_1^0,\xi_2^0)\;|\;X_i(\xi_1^0,\xi_2^0)<1\}}\frac{\partial_\xi\kappa_0}{\partial m}(\xi_1^0,\xi_2^0)\times \\ & \left(1-\frac{3}{2}X_i(\xi_1^0,\xi_2^0)+\frac{1}{2}X_i(\xi_1^0,\xi_2^0)^3\right)\left\|\frac{\partial f^0}{\partial u}\wedge\frac{\partial f^0}{\partial v}\right\| d\xi_i^0 d\xi_2^0 \end{aligned}$$

with $X_i(\xi_1^0,\xi_2^0)=\frac{\sigma_y}{2\tau\gamma}\frac{h^{2i}}{||\nabla_\xi\,\kappa_0(\xi_1^0,\xi_2^0)||}$. If X_i is close to 1, then $1-\frac{3}{2}X_i(\xi_1^0,\xi_2^0)+\frac{1}{2}X_i(\xi_1^0,\xi_2^0)^3$ is small and the relative contribution to the whole integral is small. On the contrary, if X_i is small, then the relative contribution to the integral is maximal. Consequently, the integral is dominated by the contribution of the regions where X_i is small, i.e. where the curvature gradient is large.

IV. NUMERICAL SIMULATIONS OF THE MOTION OF A LAYER OF A BINGHAM FLUID ON THE WALL OF AN AIRWAY TREE

A. Geometry

The geometry of the three generations airway tree is based on typical sizes ratio measured in the lung [13]. The root branch diameter is 1 mm and the branch size decreases at each bifurcation with the ratio $\left(\frac{1}{2}\right)^{\frac{1}{3}}$. The ratio of length over diameter is 3. Two successive branching planes form an angle of 90 degrees between each other. The CAD geometry for GMSH is automatically built using Octave, STL surface meshes are generated using GMSH [2]. Visual details are given in Fig. 5.

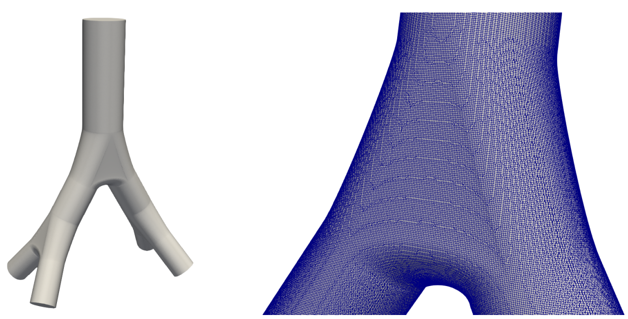

FIG. 3. The geometry and its surface mesh used in the simulations.

The curvature is computed from the surface divergence $k_0 = \text{div}_S(\boldsymbol{n})$ of the inwards normals using boundary finite elements.

Actually, a (reasonably) crude mesh brings a good characterization of the main features of a bifurcation but will affect the quality of the variables computed with the finite elements method. On the contrary, an extremely fine mesh brings high quality estimations with the finite elements method but brings noise on the curvature that is not meaningful to our approach. Thus, the curvature is smoothed in order to allow the use of a mesh that is fine enough for the finite elements method but that is also able to catch the main geometrical features of the bifurcation without noise. The curvature is smoothed using a technique from image analysis based on the heat equation [3]. The method is based on "applying" the heat equation on the divergence of the normals to the bifurcations $k_0 = \text{div}_S(\boldsymbol{n})$. More precisely, k_0 corresponds to the initial state in the following partial differential equation:

$$\begin{cases} \dfrac{\partial k}{\partial e}(\xi,e) - D\,\triangle_S\,k(\xi,e) = 0 \text{ for } (\xi,e)\in\Omega\times]0,1] \\ k(\xi,0) = k_0(\xi) \end{cases}$$

Then, the curvature used in our work is the field k taken at the time $e = 1$, i.e. $\kappa = k(.,1)$. The resulting smooth of the curvature corresponds to a convolution of the initial curvature field with a bi-dimensional Gaussian kernel

$$K(\xi) = \frac{1}{2\pi\sigma_{\mathrm{d}}^2} e^{-\frac{|\xi|^2}{2\sigma_{\mathrm{d}}^2}}$$

with a standard deviation $\sigma_{\mathrm{d}} = \sqrt{2D}$.

We tested how the smoothing affects the mean Bingham fluid velocity in the bifurcation as a function of the mesh refinement, see Fig. 4. The degree of smoothing was then determined by the value for which the velocity was the closest for all the meshes tested, indicating that the result does not depend on the mesh size. The mesh size was fixed to 0.05 mm and the standard deviation of the smoothing to $\sigma_{\mathrm{d}} = 0.2$ mm, which corresponds to a diffusive coefficient $D = 2\ 10^{-8}$ $\mathrm{m}^2.\mathrm{s}^{-1}$. The resulting smoothed curvature field is then used as the input of the computations of the model.

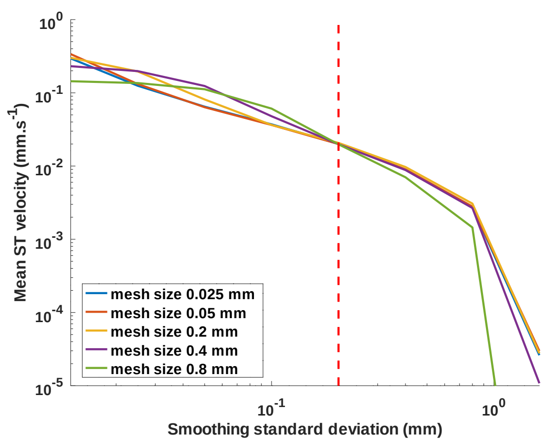

FIG. 4. Sensitivity of the mean Bingham fluid velocity (log-log) in the bifurcation relatively to the curvature smoothing (x-axis) and the mesh refinement (colored curves). The finer the mesh, the more precise is the quality of the finite elements method, but the more sensitive is the curvature to the mesh. If the smoothing standard deviation is too small, then the fluid velocity is affected by the mesh specificities, if it is too large, then the features of the bifurcation are lost. The degree of smoothing chosen is $\sigma_{\mathrm{d}} = 0.2$ mm. A smaller value induces artefacts due to the discretization in triangles of the bifurcation surface, while a larger value induces artefacts due to an over-smoothing that hides the main geometrical features of the bifurcation. The mesh size chosen was 0.05 mm, which corresponds to 186 594 triangles for meshing the bifurcation surface.

B. Numerical simulations

To study the properties of a thin layer of Bingham fluid in a 3D geometry, we used boundary finite elements within Comsol Multiphysics 3.5a.

The healthy layer thickness chosen in our work corresponds to the most frequent mean value reported in the literature: $\tau = 10$ μm [4]. Several other thickness values have been simulated to mimic pathological mucus layer, up to $\tau = 150$ μm.

We estimated the characteristic size of the domain R using the airways radii. The thickness can be considered small relatively to the curvature radius in most of the generations of the tree. We indicated in the results when this hypothesis breaks. We use the results from lubrication theory of a Bingham fluid to estimate the main component of the thin Bingham fluid layer velocity.

Embedded capability of Comsol Multiphysics 3.5a are used to compute the tangential and normal vectors of a surface. Moreover, these vectors define an orthonormal local basis and the metric tensors $g^{(i,j)}$ and $g_{(i,j)}$ are equal to the identity matrix. As a consequence, the dominant velocities of the Bingham layer averaged over its thickness express as

$$\begin{cases} u_m^1(\xi_1,\xi_2) = -\frac{1}{2\mu}\frac{\partial p_L}{\partial \xi_1}\hat{Z}^2(\xi_1,\xi_2)\left(1-\frac{\hat{Z}(\xi_1,\xi_2)}{3(\tau+\eta)}\right) + O(U\epsilon) \\ u_m^2(\xi_1,\xi_2) = -\frac{1}{2\mu}\frac{\partial p_L}{\partial \xi_2}\hat{Z}^2(\xi_1,\xi_2)\left(1-\frac{\hat{Z}(\xi_1,\xi_2)}{3(\tau+\eta)}\right) + O(U\epsilon) \\ u_m^3(\xi_1,\xi_2) = O(U\epsilon) \\ \hat{Z}(x,y) = \max\left(0, \tau+\eta(\xi_1,\xi_2) - \frac{\sigma_y}{||\nabla_\xi\, p_L(\xi_1,\xi_2)||}\right) \end{cases}$$

We use the embedded surface derivatives in Comsol Multiphysics to compute the surface divergence of the normal $\boldsymbol{n}$ to the surface. The mean curvature of the surface of the airway walls is then $\kappa = \frac{1}{2}\mathrm{div}_\xi(\boldsymbol{n})$. To avoid a noisy curvature due to the meshing of the surface, the resulting curvature is smoothed locally using a kernel whose width is determined in section IV A of this Supplemental Materials.

We assume that the air pressure in the airways is 0. Then, the Laplace pressure is then computed as $p_L = -2\gamma\kappa$, with γ the surface tension.

Finally, we use again the embedded surface derivatives in Comsol Multiphysics to compute the derivatives of p_L, $\frac{\partial p_L}{\partial \xi_1}$ and $\frac{\partial p_L}{\partial \xi_1}$ along the tangential directions to the airway walls.

V. ESTIMATING THE ORIENTATION OF CILIA VELOCITY

The mucociliary motion of mucus was mimicked using a velocity at the airways wall with an amplitude $v_{\text{cilia}} = 50\ \mu m.s^{-1}$. The directions of the mucocilliary motion were determined by the directions of the gradient of a Laplacian L field with the following boundary conditions: $L = 1$ at the opening of the largest airway of the bifurcation; $L = 0$ at the opening of the smallest airways of the bifurcation. No L flow was allowed through the wall of the tree. The wall gradient of such a field is smooth, tangent to the wall and parallel to the centerlines of the tree. We assumed that the velocity induced on mucus by mucocilliary transport is

$$\boldsymbol{v}_{\text{cilia}} = v_{\text{cilia}} \times \frac{\nabla L}{||\nabla L||}$$

Another way for estimating the velocity field induced by mucocilliary clearance is proposed in [6]. The properties

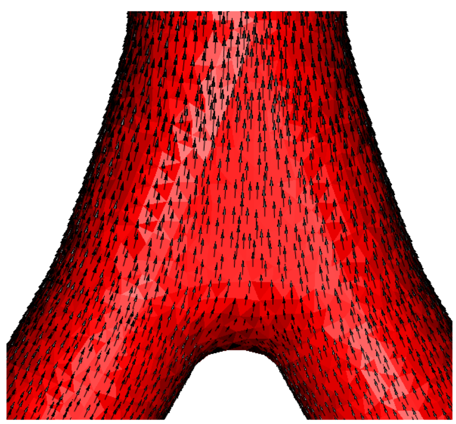

FIG. 5. Details of a bifurcation to show the direction of the motion of mucus due to cilia predicted by our model based on the gradient of a Laplacian field.

of the field obtained by our method and and in [6] are very close. The method proposed here allows to compute a velocity wall field without computing the centerlines of the tree, which can be useful for complex geometries.

As discussed in [4], the assumption of a generation-independent velocity amplitude for the mucus layer is not compatible with a constant mucus layer thickness throughout the tree. Indeed, if we consider a branch in generation i with radius r_i that bifurcates into two branches in generation $i+1$ with radii $r_{i+1} = hr_i$, we can relate the mucus layer thicknesses τ_i and τ_{i+1} between the two generations:

$$\underbrace{2\pi r_i\ \tau_i\ v_{\text{cilia}}}_{\text{outflow of branch } i} = \underbrace{2\times 2\pi r_{i+1}\ \tau_{i+1}\ v_{\text{cilia}}}_{\text{outflow of branches } i+1} \longrightarrow \tau_i = 2h\ \tau_{i+1} \simeq 1.59\ \tau_{i+1}$$

Thus, the small differences in term of mucus layer thicknesses between the bronchi generations is likely to result from a regulation by other mechanisms, which are not well described as of today [4]. The way mucociliary clearance is mimicked in this study does not account for such potential other regulation mechanisms.

---

[1] N. J. Balmforth and R. V. Craster. A consistent thin-layer theory for Bingham plastics. *Journal of Non-Newtonian Fluid Mechanics*, 84(1):65–81, July 1999.

[2] C. Geuzaine and J.-F. Remacle. Gmsh: A 3-D finite element mesh generator with built-in pre-and post-processing facilities. *International Journal for Numerical Methods in Engineering*, 79(11):1309–1331, 2009.

[3] F. Guichard, L. Moisan, and J.-M. Morel. A review of P.D.E. models in image processing and image analysis. *J. Phys. IV France*, 12(1):137–154, Mar. 2002. Publisher: EDP Sciences.

[4] C. Karamaoun, B. Sobac, B. Mauroy, A. V. Muylem, and B. Haut. New insights into the mechanisms controlling the bronchial mucus balance. *PLOS ONE*, 13(6):e0199319, June 2018.

[5] C. Karamaoun, B. Sobac, B. Mauroy, A. Van Muylem, and B. haut. New analysis of the mechanisms controlling the bronchial mucus balance. In *27th Canadian Congress of Applied Mechanics*, Sherbrooke,, Canada, June 2019.

[6] M. Manolidis, D. Isabey, B. Louis, J. B. Grotberg, and M. Filoche. A Macroscopic Model for Simulating the Mucociliary Clearance in a Bronchial Bifurcation: The Role of Surface Tension. *Journal of Biomechanical Engineering*, 138(12):121005, Nov. 2016.

[7] B. Mauroy, C. Fausser, D. Pelca, J. Merckx, and P. Flaud. Toward the modeling of mucus draining from the human lung: role of the geometry of the airway tree. *Physical Biology*, 8(5):056006, Oct. 2011.

[8] B. Mauroy, M. Filoche, J. S. Andrade, and B. Sapoval. Interplay between geometry and flow distribution in an airway tree. *Physical Review Letters*, 90:148101, Apr. 2003.

[9] B. Mauroy, M. Filoche, E. R. Weibel, and B. Sapoval. An optimal bronchial tree may be dangerous. *Nature*, 427(6975):633–636, Feb. 2004.

[10] B. Mauroy, P. Flaud, D. Pelca, C. Fausser, J. Merckx, and B. R. Mitchell. Toward the modeling of mucus draining from human lung: role of airways deformation on air-mucus interaction. *Front. Physiol.*, 6, 2015.

[11] F. Noël, C. Karamaoun, J. A. Dempsey, and B. Mauroy. The origin of the allometric scaling of lung's ventilation in mammals. *arXiv:2005.12362 [q-bio]*, in revision in PCI MCB, Aug. 2020. arXiv: 2005.12362.

[12] B. Sobac, C. Karamaoun, B. Haut, and B. Mauroy. Allometric scaling of heat and water exchanges in the mammals' lung. *arXiv:1911.11700 [physics]*, Dec. 2019. arXiv: 1911.11700.

[13] M. H. Tawhai, P. Hunter, J. Tschirren, J. Reinhardt, G. McLennan, and E. A. Hoffman. CT-based geometry analysis and finite element models of the human and ovine bronchial tree. *J. Appl. Physiol.*, 97(6):2310–2321, Dec. 2004.

[14] E. R. Weibel. *The Pathway for Oxygen: Structure and Function in the Mammalian Respiratory System.* Harvard University Press, 1984.

[15] E. R. Weibel, A. F. Cournand, and D. W. Richards. *Morphometry of the Human Lung.* Springer, 1 edition edition, Jan. 1963.